International Journal of Information, Control and Computer Sciences
ISSN: 2517-9942
Vol:9, No:2, 2015

# Design of Direct Power Controller for a High Power Neutral Point Clamped Converter Using Real Time Simulator

Amin Zabihinejad, Philippe Viarouge

***Abstract*—In this paper, a direct power control (DPC) strategies have been investigated in order to control a high power AC/DC converter with time variable load. This converter is composed of a three level three phase neutral point clamped (NPC) converter as rectifier and an H-bridge four quadrant current control converter. In the high power application, controller not only must adjust the desire outputs but also decrease the level of distortions which are injected to the network from the converter. Regarding to this reason and nonlinearity of the power electronic converter, the conventional controllers cannot achieve appropriate responses. In this research, the precise mathematical analysis has been employed to design the appropriate controller in order to control the time variable load. A DPC controller has been proposed and simulated using Matlab/ Simulink. In order to verify the simulation result, a real time simulator- OPAL-RT- has been employed. In this paper, the dynamic response and stability of the high power NPC with variable load has been investigated and compared with conventional types using a real time simulator. The results proved that the DPC controller is more stable and has more precise outputs in comparison with conventional controller.**

***Keywords*—Direct Power Control, Three Level Rectifier, Real Time Simulator, High Power Application.**

## I. Introduction

MULTILEVEL converters [1], [2] are one of the best solutions to use in the high power applications. Recently, the demands for high power converters in order to connect to the grid for renewable energy and other applications make using multi-level converters topology more suitable than two-level PWM rectifier [3]. Using multi-level converters will leads to the lower voltage stress across semiconductor devices, lower switching frequency and less harmonic distortion in AC side. Additionally, regarding to design the appropriate controller, multi-level converters provide more adjustable states. As shown in Fig. 1, a high power NPC rectifier is connected to the grid via DY three-phase transformer. A capacitor bank is placed at the rectifier output. The NPC rectifier supplies a time variable load. The H-bridge converter provides the current of the load which is adjusted with a current controlled controller. The current of the load changes from 300A to 6000A in less than 0.3 second. The extreme change of load current affects the DC link voltage and drops it. In this condition, conventional controller does not have satisfied performance. Also, the controller must set the reactive power to zero to decrease the mis-effect of converter on the grid, especially in the low switching frequencies. In high power applications, the switch losses will be very important. It is a significant limitation in order to increase the power of the converters. Decreasing the switching frequency is one of the prevalent tasks in order to decrease the switch losses. This limitation forces us to choose a low switching frequency- 1 KHz - for this application. Among various control strategies, the direct power control (DPC) was chosen based on its high dynamic performance, algorithm simplicity (without need to coordinate transformation, internal current loops, and modulator), and robust behavior against system variations due to the hysteresis controller used for the instantaneous active and reactive power control [1], [2]. A real time simulator has been employed to verify the simulation results. The real time simulator is composed of software and hardware section. OPAL-RT Company introduces the RT-Lab as the software which compiles the model in order to implement in the hardware section. It is fully integrated with Matlab/Simulink and compiles the generated model in the sympower library. OP4500 is a real time hardware simulator which is used to execute the power electronic model. OP4500 utilize the exact IGBT and Diode and power system elements model using FPGA technology. Also other parts of simulation will execute by the powerful CPUs of the OP4500.

A. Zabihinejad is PHD student with Electrical Engineering Department, Laval University, Quebec city, QC, Canada where he is working in LEEPCI labratory(amin.zabihinejad.1@ulaval.ca).

P. Viarouge is Professor with the Department of Electrical Engineering, Laval University, Quebec City, QC, Canada, where he is currently working in the research laboratory Laboratoire dlectrotechnique, lectronique de Puissance et Commande Industrielle.(philippe.viarouge@gel.ulaval.ca).

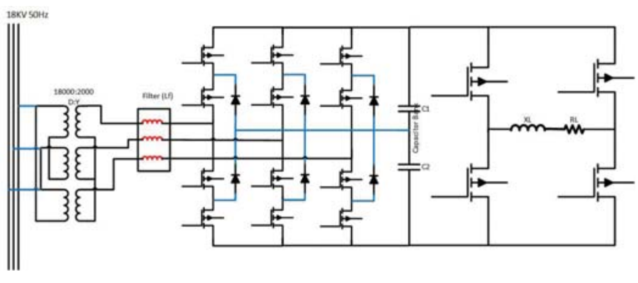


Fig. 1. NPC rectifier with current controlled load

The Real time simulator helps us to execute the very complex power electronic model in real time to evaluate the dynamic setting of the controller and power quality of the converter [4]. It can be a valuable step in order to design the high power converters which are very expensive and time consuming to implement.

## II. Mathematical Model of Three Phase Three Level Rectifier

A neutral point clamped rectifier has been shown in the Fig. 2. Based on KVL, the voltage relations of input circuit are written as below:

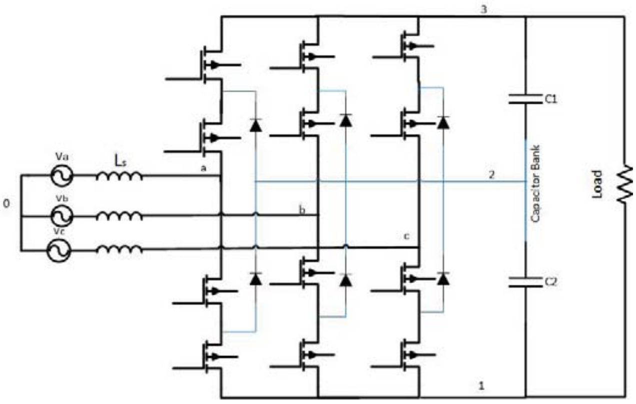


Fig. 2. Neutral point clamped rectifier

$$\begin{aligned} V_a &= i_a R_s + L_s p i_a + V_{a0} \\ V_b &= i_b R_s + L_s p i_b + V_{b0} \\ V_c &= i_c R_s + L_s p i_c + V_{c0} \end{aligned} \tag{1}$$

For node a, there are three voltage states. The point a connects to "3" if $S_{1a}\ and\ S_{2a}$ is ON. This state is $\mu_{a3}$. Similarly, $\mu_{a2}$ is for "2" and $\mu_{a1}$ is for "1" [5].

$$\begin{bmatrix} V_{a0} \\ V_{b0} \\ V_{c0} \end{bmatrix} = \begin{bmatrix} \mu_{a3} & \mu_{a2} & \mu_{a1} \\ \mu_{b3} & \mu_{b2} & \mu_{b1} \\ \mu_{c3} & \mu_{c2} & \mu_{c1} \end{bmatrix} \begin{bmatrix} V_{30} \\ V_{20} \\ V_{10} \end{bmatrix} \tag{2}$$

It is obvious that at any time, just one of this states can be ON to avoid the capacitors shorting. Therefore, for each phase:

$$\mu_3 + \mu_2 + \mu_1 = 1 \tag{3}$$

Therefor for phase A

$$\mu_{a2} = 1 - \mu_{a3} - \mu_{a1} \tag{4}$$

By substituting in the output voltage equation:

$$V_{a0} = \mu_{a3} V_{c1} - \mu_{a1} V_{c2} + V_{20} \tag{5}$$

Therefore,

$$\begin{bmatrix} V_{a0} \\ V_{b0} \\ V_{c0} \end{bmatrix} = \begin{bmatrix} \mu_{a3} & -\mu_{a1} & 1 \\ \mu_{b3} & -\mu_{b1} & 1 \\ \mu_{c3} & -\mu_{c1} & 1 \end{bmatrix} \begin{bmatrix} V_{c1} \\ V_{c2} \\ V_{20} \end{bmatrix} \tag{6}$$

By composing the input and output equations, the new equations will be generated [5].

$$\begin{aligned} V_a &= i_a R_s + L_s p i_a + \mu_{a3} V_{c1} - \mu_{a1} V_{c2} + V_{20} \\ V_b &= i_b R_s + L_s p i_b + \mu_{b3} V_{c1} - \mu_{b1} V_{c2} + V_{20} \\ V_c &= i_c R_s + L_s p i_c + \mu_{c3} V_{c1} - \mu_{c1} V_{c2} + V_{20} \end{aligned} \tag{7}$$

The $\mu_{a3}, \mu_{a2}, \mu_{a1}$ are defined as below: [6]

$$\begin{aligned} \mu_{a1} &= \tfrac{1}{3}(M_{a1}+1) \\ \mu_{a2} &= \tfrac{1}{3}(M_{a2}+1) \\ \mu_{a2} &= \tfrac{1}{3}(M_{a2}+1) \\ \mu_{a3} &= \tfrac{1}{3}(M_{a3}+1) \end{aligned} \tag{8}$$

In the output of the rectifier, the currents $I_1,\ I_2\ and\ I_3$are as below:

$$\begin{bmatrix} I_1 \\ I_2 \\ I_3 \end{bmatrix} = \begin{bmatrix} \mu_{a3} & \mu_{a2} & \mu_{a1} \\ \mu_{b3} & \mu_{b2} & \mu_{b1} \\ \mu_{c3} & \mu_{c2} & \mu_{c1} \end{bmatrix} \begin{bmatrix} I_a \\ I_b \\ I_c \end{bmatrix} \tag{9}$$

The output DC current of the rectifier is:

$$\begin{aligned} C_1 p V_{c1} &= -I_{dc} + \mu_{a3} I_a + \mu_{b3} I_b + \mu_{c3} I_c \\ C_2 p V_{c2} &= -(I_{dc} + \mu_{a3} I_a + \mu_{b3} I_b + \mu_{c3} I_c) \end{aligned} \tag{10}$$

Now, we have five state variables and five state equations in ABC system regarding to the input and output circuits of the rectifier.

To decrease the number of variable and achieve the simpler controller, the equations were transferred from ABC to D-Q synchronous reference frame system. This transformation is done using$T(\theta)$ where, $\theta = 2\pi f_s$.

Also, the modulation indexes $(\mu)$ are transferred to D-Q system. Using the synchronous reference frame transfer function, our state equation will be as below:

$$\begin{cases} pI_q = \frac{1}{L_s}(V_q - R_s I_q - \omega_e L_s I_d - V_{c1}\mu_{q3} + V_{c2}\mu_{q1}) \\ pI_d = \frac{1}{L_s}(V_d - R_s I_d + \omega_e L_s I_q - V_{c1}\mu_{d3} + V_{c2}\mu_{d1}) \\ pV_{c1} = -\frac{1}{C_1}\left[I_{dc} - \frac{3}{2}(\mu_{q3} I_q + \mu_{d3} I_d)\right] \\ pV_{c2} = -\frac{1}{C_2}\left[I_{dc} + \frac{3}{2}(\mu_{q1} I_q + \mu_{d1} I_d)\right] \end{cases} \tag{11}$$

Where$V_{dc} = V_{c1} + V_{c2}$ , $V_q = V_s$ , $V_d = 0$ , $I_{dc} = I_L$;

## III. Direct Power Control Concept

In 1998, Noguchi [2] has proposed the basic principle of the Direct Power Control (DPC) which is based on the well-known Direct Torque Control (DTC) for induction machines. In the DPC, the active and reactive powers are utilized instead of the torque and flux amplitude used as the controlled output in the DTC [2], [6]. Recently, different concepts of DPC has been proposed by researchers. The main goal of these concepts is achieving an appropriate algorithm in order to select the switching states from a switching table based on the errors present in the active and reactive powers, which are limited by a hysteresis band.

The most important advantages of the DPC strategies are the simplicity of calculation, high dynamic response, it's robustness regarding to system variations and the possibility to control the active and reactive power in the same time.

Three-level converters, can generate a two-layer hexagon centred at the origin of the ($\alpha$, $\beta$) plane and a zero voltage vector at the origin of the plane. The voltage vectors of the NPC depends only on the leg states of the rectifier. The principle of operation shows that it can generate twenty seven space vectors. Regarding to reduce the current distortion, the desired voltage vector is to be assembled of only direct adjacent possible switching states of the converter [7].

As shown in Fig.Fig. 3, three level converter generates eighteen possible non-zero vectors where two-level converters just are able to generate six voltage vectors and two zero vectors. Base on their magnitudes, the space voltage vectors usually are divided into four groups as below Table:

TABLE I
DIFFERENT TYPES of VOLTAGE VECTOR of the NPC

| | |
|---|---|
| zero voltage vectors | V0 |
| small voltage vectors | V1 , V4 ,V7 , V10 , V13 , V16 |
| middle voltage vectors | V3 , V6 , V9 ,V12 , V15 , V18 |
| large voltage vectors | V2 , V5 , V8 , V11 ,V14 , V17 |

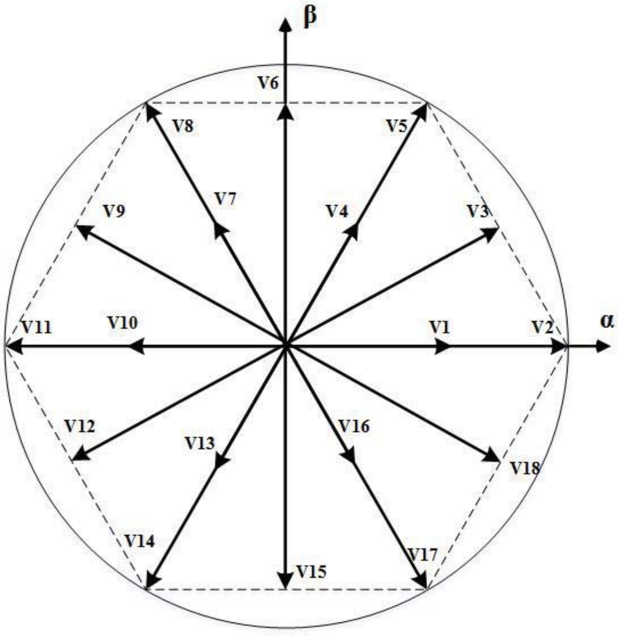


Fig. 3. Space voltage vectors of a three-level rectifier

The second significant reason to use the multilevel converter is the possibility to work with lower switching frequency whiles the output is generated with higher switching frequency. This advantage is very important in order to design high power application where the value of the switching losses is the most important point in the design process.

Researchers proposed two methods to calculate the active and reactive power in the DPC strategy. In the first method, the measured line currents ia, ib, and phase voltages ua, ub are used in the power calculation. Using the stationary coordinate system, the transient value of active and reactive power can be estimated for sinusoidal and balanced phase voltage as below:

$$P = \tfrac{3}{2}(u_a i_a + u_\beta i_\beta)$$
$$Q = \tfrac{3}{2}(u_a i_\beta - u_\beta i_a) \tag{12}$$

In the second approach, the Virtual Flux strategy [2] has been proposed to equalize the phase voltage and the AC side inductors to be quantities same as a virtual AC motor. The mathematical model of three-level rectifier in (d, q) synchronous plane based on DPC is described as, [8].

$$\tfrac{dP}{dt} = \tfrac{3V_s}{L_s}(u_{sd} - u_{sr})$$
$$\tfrac{dQ}{dt} = 3u_{sd}.\tfrac{u_{rd}}{L_s} \tag{13}$$

Where, $u_{sd}, u_{rd}$ are the source voltage and rectifier voltage in the synchronous plane. The phase voltage of the phase a, is aligned with the d axis.

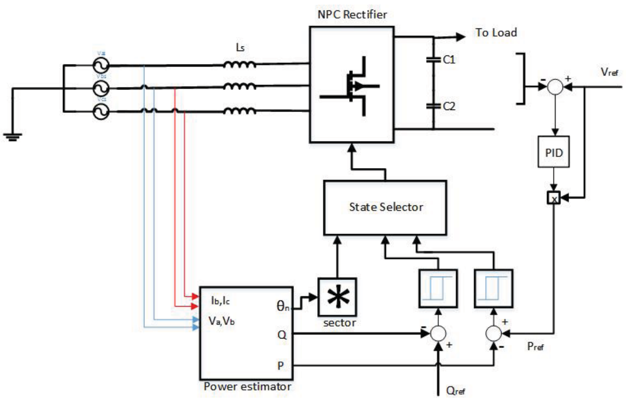


Fig. 4. The diagram of the DPC controller

The diagram of the DPC controller has been shown in Fig. 4. The input parameter are the source currents and voltages. Also, the DC link voltage is the feedback parameter which is compared with the setpoint and passed through the PID to generate the reference of the active power. Also, to increase the power coefficient, the setpoint of the reactive power will set to zero.

Another important parameter in DPC concept is the angel of space vector ($\theta$). Regarding to 12 section which is seen in Fig. 3, the value of $\theta$ is defined as below:

$$(n-1)\,\tfrac{\pi}{6} < \theta < n\tfrac{\pi}{6}\ ,\quad 1 < n < 12 \tag{14}$$

## IV. Switching Strategy of DPC

Different switching strategies have been proposed in order to increase the dynamic response, decrease the harmonics and reactive power [9]. The more effective strategy regarding to dynamic response has been proposed as below [9].

| $\triangle P$ | $< -h$ | $-h >, < h$ | $> h$ |
|---|---|---|---|
| $d_P$ | 1 | 2 | 3 |

| $\triangle P$ | $< -k$ | $-k >, < k$ | $> k$ |
|---|---|---|---|
| $d_Q$ | 1 | 2 | 3 |

The appropriate switching table for the three first sectors has been proposed in table II. For other sectors selecting the vector will be the same. In order to increase the capacity of converter to absorb more energy in regeneration time, we modified the negative section of active power into two section as seen in Table II.

TABLE II
The Switching Table for Three First Sectors

| $d_P$ | $d_Q$ | $\theta_1$ | $\theta_2$ | $\theta_3$ |
|---|---|---|---|---|
| | 3 | 7 | 9 | 10 |
| 3 | 2 | 10 | 10 | 13 |
| | 1 | 13 | 16 | 16 |
| | 3 | 6 | 8 | 9 |
| 2 | 2 | 4 | 4 | 7 |
| | 1 | 1 | 1 | 4 |
| | 3 | 3 | 5 | 6 |
| 1, $dv < -v_0$ | 2 | 3 | 5 | 6 |
| | 1 | 2 | 3 | 5 |
| | 3 | 17 | 18 | 2 |
| 1, $dv > -v0$ | 2 | 17 | 18 | 2 |
| | 1 | 15 | 17 | 18 |

where $dv = V_{ref} - V_{DC\ link}$.

## V. Simulation Results

In this research, we utilize two different approaches to evaluate the controller's performance. The DPC concept has been verified by Matlab/Simulink and the real time simulator. The circuit parameters in the Fig. 1, has been listed in the Table III.

TABLE III
The Value of the Circuit Parameters

| Vs (rms) | Rs (ohm) | Ls (mH) | $R_L$(ohm) | $L_L$(H) | $f_{SW}$(Hz) |
|---|---|---|---|---|---|
| 2000 | 0.001 | 0.8 | 0.28 | 0.1 | 1000 |

The reference value of DC link voltage of the rectifier which is connected to two 600mF capacitors is set to 5000V as the given value. Also, the reference value of reactive power is set to zero to let the inverter working in the unity power factor.

### A. Step Response

In the first section, the step response test has been simulated. The setpoint of the DC link has been changed from 4500V to 5000V. The Fig.3 show the actual value and setpoint value of the DC link voltage. The Fig. 5 and 6, shows the ac source currents and active and reactive power, respectively. The unity power factor condition of the rectifier is achieved. As seen in Fig. 7, the DPC strategy choose directly the appropriate voltage vector to reduce the control error, providing very fast power control in active power, while, the reactive power keeps zero with a little oscillation for response the step.

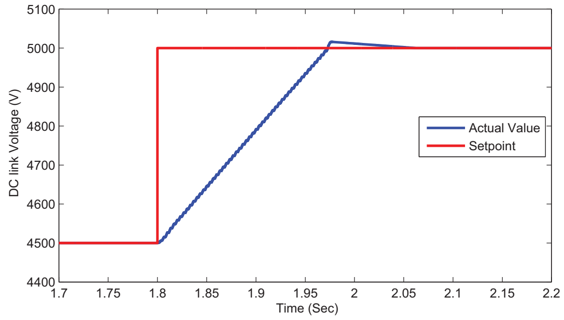


Fig. 5. Step response of DC link voltage

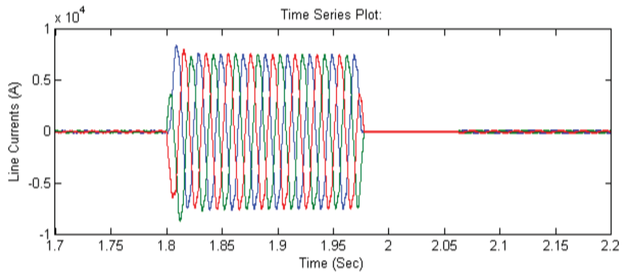


Fig. 6. The Phase Currents in step response

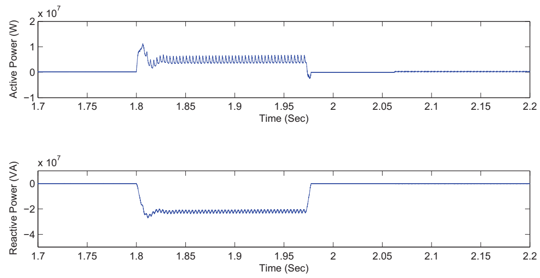


Fig. 7. Active and reactive power in step response

### B. Load Current Control

In our application, the load of the NPC is a RL branch which is supplied by an H-bridge converter. The current of the RL branch is controlled using a current controller. The waveform of the reference current is the same of a narrow pulse with the high value in the top. The intense load variation in a short period of time is a difficult situation in order to design the appropriate controller. On the other hand, NPC rectifier must work as bidirectional converter. The conventional controllers cannot bring suitable response in this condition.

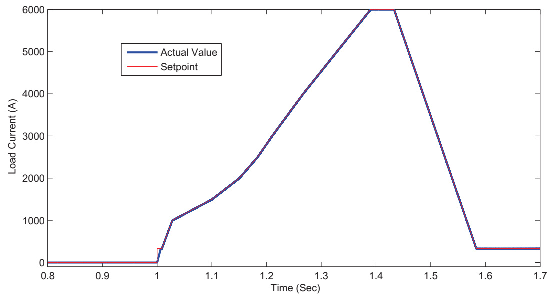


Fig. 8. Actual and reference current value of the load

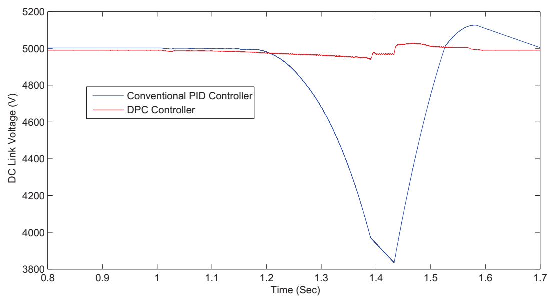


Fig. 9. DC link voltage using DPC and conventional controller

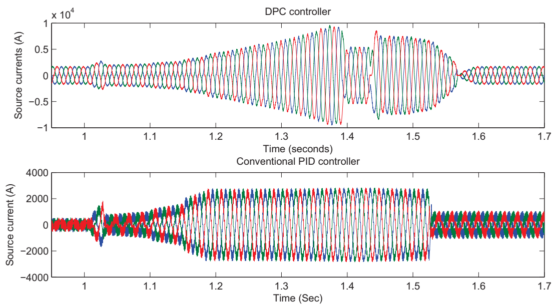


Fig. 10. AC source currents in the DPC and conventional controller

The actual and reference value of the load current has been shown in the Fig. 8. The variation of DC link voltage has been compared in Fig. 9. As shown in the Fig.9, the maximum ripple of the voltage is less than 1% for 6000 A at the output where the case of conventional controller, the voltage ripple is more than 26%. Also, the AC source currents for DPC and conventional controller have been shown in the Fig. 10. It is clear that conventional controller does not have satisfied action in the case of intense variations of the load current.

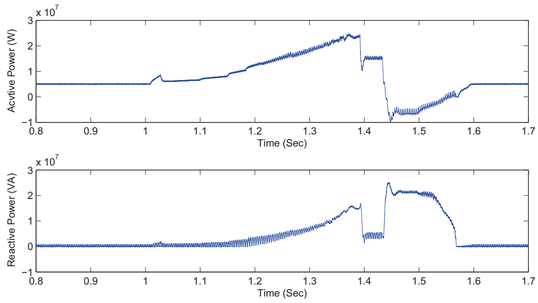


Fig. 11. Active and reactive power in DPC control

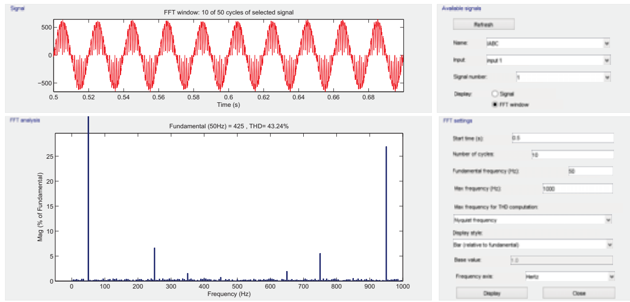


Fig. 12. The steady state source current and FFT analysis for DPC controller

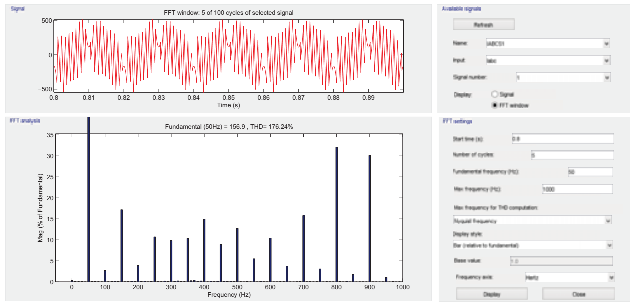


Fig. 13. The steady state source current and FFT analysis for conventional controller

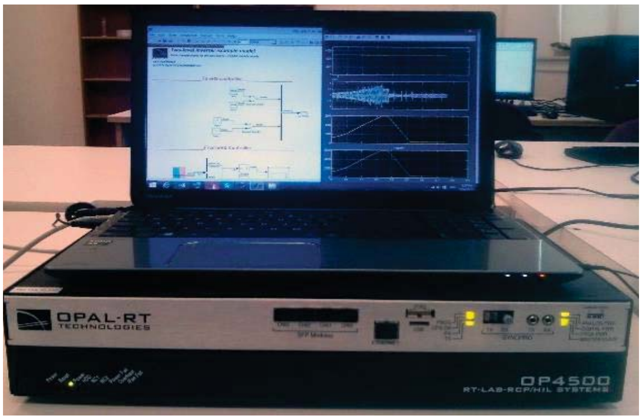


Fig. 14. OP4500, OPAL-RT real time simulator and RT-Lab software

Fig. 11 proves the bidirectional property of NPC rectifier. When the DC current increases, the active power is stored in the inductor, therefore, the input active power increases. When the current decreases, the active power must be came back to the source very fast. Therefore, the input active power will be negative. Also, because of inductive load, the reactive power will increase.

Fig. 12 and 13 show the FFT analysis of the AC source current in the steady-state for DPC and conventional PID control strategies respectively. It is obvious that the DPC controller output has much less harmonics and oscillations compared to conventional type. The THD value is less than 43.5% using DPC controller whether in the case of conventional PID, the THD value is more than 175%. Therefore, the converter with DPC controller has more quality of power in comparison with conventional controller and it will have less mis-effects on the grid and does not need to use complex filter to decrease the harmonics.

## VI. Implementation by Real Time Simulator

Real-time simulator (RTS) is a valuable tool of virtual prototyping used to study the dynamics of a physical system prior to actual hardware development [10]. Recently, RTS has been utilized by engineers in various industries such as aviation [8], power systems [8], networking [11], automotive [12], traffic management [13], and medicine [14]. The implementation of power electronic converters is very expensive and time consuming, especially in high power application. The real time simulator is known as very effective approach to verify the model dynamics and controller setting validation.

In this research, OP4500, a real time simulator from OPAL-RT Company, has employed to evaluate the controller design. The RTSs often have two main sections; software and hardware. The software is a computer program which connect the simulation files to the hardware. OPAL-RT introduces the RT-Lab as software that receive the Matlab/Simulink files and translate them in order to load and execute. The OPAL-RT hardware is composed of two main sections, CPU and FPGA. The power system and power electronic components are directly implemented in FPGA section. The RT-LAB uses the precise model of IGBT, diodes and other power electronic components. The control system components is executed by CPU section. All simulation sectors must execute in real time. Fig. 14 shows the OP4500 and the setup which is prepared for this project. The results of the simulation using RTS have been shown in Fig. 15, 16 and 17. Fig. 15 shows the actual and reference current value of the load. Fig. 16 shows the DC link voltage in full load using DPC controller. The waveform of the voltage in RTS and Simulink are the same except the high frequency spikes. RTS uses the more precise model for IGBTs. The oscillations which are seen in the voltage waveform are visible when the exact IGBT model is used. Fig. 17 shows the three phase source currents in the full load condition. Also, Fig. 18 shows the steady-state current of the phase A and its FFT analysis. The FFT analysis shows that the THD value is more than the value in the simulation. This measurement is very important in order to design the harmonic filter for the converters.

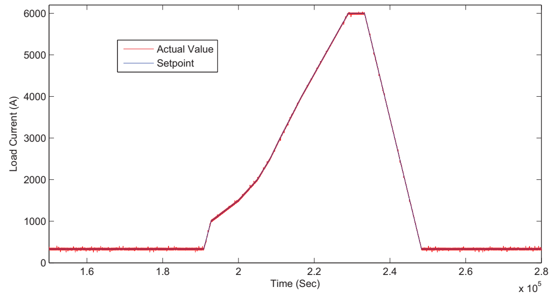


Fig. 15. Actual and reference value of load current using RTS

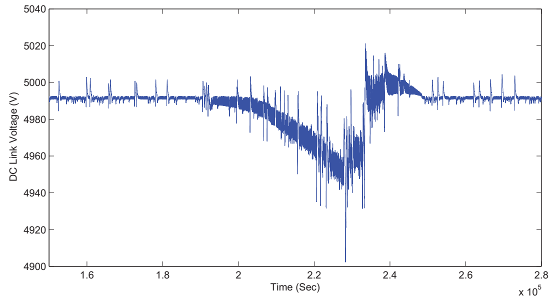


Fig. 16. DC link voltage in full load using RTS

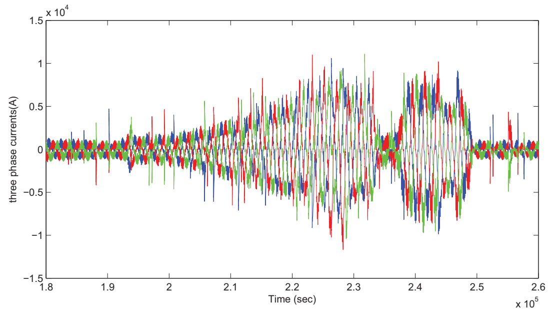


Fig. 17. The source currents in full load using RTS

## VII. Conclusion

In this paper, the validity of a proposed DPC control strategy for a high power NPC rectifier with a time variable load has been investigated using two different approaches. The concept of DPC control is proved by the Matlab/Simulink and real time simulator results. Real time simulator is an effective and valuable approach to demonstrate the validation of the controller setting in power electronic design especially in high power application [8], [11]–[14]. The results of DPC controller has been compared with conventional PID controller. The simulation results proved that the DPC controller has better dynamic response, less ripple, harmonics and voltage drop.

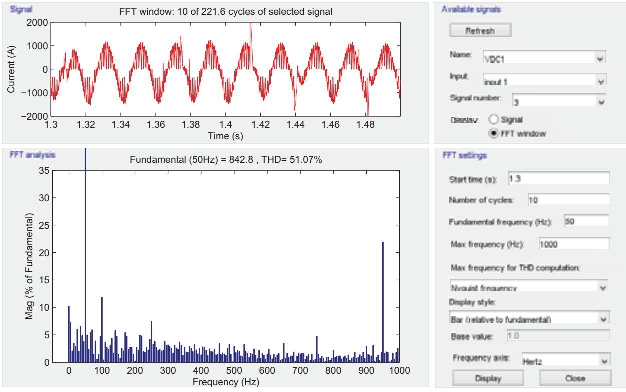


Fig. 18. The steady state current source and FFT analysis of the RTS output

Implementation of high power application is very expensive and risky. Real time simulator help us to evaluate the simulation results. The OP4500 - OPAL-RT simulator - was used in this research. The results with RTS proved the simulation results.

## Acknowledgment

The authors would like to acknowledge the active participation and financial support of the OPAL-RT Company and department of electrical engineer of Laval University.

## References

[1] M. Malinowski, M. P. Kazmierkowski, S. Hansen, F. Blaabjerg, and G. Marques, "Virtual-flux-based direct power control of three-phase pwm rectifiers," *Industry Applications, IEEE Transactions on*, vol. 37, no. 4, pp. 1019–1027, 2001.

[2] T. Noguchi, H. Tomiki, S. Kondo, and I. Takahashi, "Direct power control of pwm converter without power-source voltage sensors," *Industry Applications, IEEE Transactions on*, vol. 34, no. 3, pp. 473–479, 1998.

[3] L. A. Serpa and J. W. Kolar, "Virtual-flux direct power control for mains connected three-level npc inverter systems," in *Power Conversion Conference-Nagoya, 2007. PCC'07*. IEEE, 2007, pp. 130–136.

[4] M. I. A. Zabihinejad, "Modeling and implementation of generator and network simulator for static exciters using matlab and labview," *Journal of Applied Sciences*, vol. 11, no. 3, 2011.

[5] M. Fracchia, T. Ghiara, M. Marchesoni, and M. Mazzucchelli, "Optimized modulation techniques for the generalized n-level converter," in *Power Electronics Specialists Conference, 1992. PESC'92 Record., 23rd Annual IEEE*. IEEE, 1992, pp. 1205–1213.

[6] F. Z. Peng, "A generalized multilevel inverter topology with self voltage balancing," in *Industry Applications Conference, 2000. Conference Record of the 2000 IEEE*, vol. 3. IEEE, 2000, pp. 2024–2031.

[7] Z. Yingchao, Z. Zhengming, Z. Yongchang, L. Ting, and Y. Liqiang, "The virtual flux oriented control of three-level neutral point clamped pwm rectifier," in *Electrical Machines and Systems, 2007. ICEMS. International Conference on*. IEEE, 2007, pp. 22–27.

[8] S. Zheng, S. Zheng, J. He, and J. Han, "An optimized distributed real-time simulation framework for high fidelity flight simulator research," in *Information and Automation, 2009. ICIA'09. International Conference on*. IEEE, 2009, pp. 1597–1601.

[9] W. Wenjun, Z. Yanru, and W. Jianjun, "The comparative study of different methods about constructing switching table in dpc for three-level rectifier," in *Power Electronics for Distributed Generation Systems (PEDG), 2010 2nd IEEE International Symposium on*. IEEE, 2010, pp. 314–319.

[10] M. Monga, "Real-time simulation of dynamic vehicle models using high performance reconfigurable computing platforms," 2010.

[11] X. Xiaobo, Z. Kangfeng, Y. Yixian, and X. Guoai, "A model for real-time simulation of large-scale networks based on network processor," in *Broadband Network & Multimedia Technology, 2009. IC-BNMT'09. 2nd IEEE International Conference on*. IEEE, 2009, pp. 237–241.

[12] M. J. Tavernini, B. A. Niemoeller, and P. T. Krein, "Real-time low-level simulation of hybrid vehicle systems for hardware-in-the-loop applications," in *Vehicle Power and Propulsion Conference, 2009. VPPC'09. IEEE*. IEEE, 2009, pp. 890–895.

[13] J. Maroto, E. Delso, J. Felez, and J. M. Cabanellas, "Real-time traffic simulation with a microscopic model," *Intelligent Transportation Systems, IEEE Transactions on*, vol. 7, no. 4, pp. 513–527, 2006.

[14] M. Lerotic, S.-L. Lee, J. Keegan, and G.-Z. Yang, "Image constrained finite element modelling for real-time surgical simulation and guidance," in *Biomedical Imaging: From Nano to Macro, 2009. ISBI'09. IEEE International Symposium on*. IEEE, 2009, pp. 1063–1066.